doi:10.1246/cl.2011.1357
Published on the web November 19, 2011

p-Aminophenyl Alkyl Ether-based ^{19}F MRI Probe for Specific Detection and Imaging of Hypochlorite Ion

Tomohiro Doura,[1] Qi An,[1] Fuminori Sugihara,[2] Tetsuya Matsuda,[2] and Shinsuke Sando*[1,3]
[1]*INAMORI Frontier Research Center, Kyushu University, 744 Motooka, Nishi-ku, Fukuoka 819-0395*
[2]*Department of Systems Science, Graduate School of Informatics, Kyoto University, 36-1 Yoshida-Honmachi, Sakyo-ku, Kyoto 606-8501*
[3]*PRESTO, Japan Science and Technology Agency, 4-1-8 Honcho, Kawaguchi, Saitama 332-0012*

(Received September 1, 2011; CL-110730; E-mail: ssando@ifrc.kyushu-u.ac.jp)

We report a ^{19}F MRI probe for the specific detection and imaging of $^{-}$OCl. Our designed probe, having *p*-aminophenyl alkyl scaffold, reacted expeditiously with $^{-}$OCl to produce a trifluoroethanol. Concomitant with the reaction, the ^{19}F chemical shift changed by 2.6 ppm, allowing the visualization of $^{-}$OCl-dependent probe-to-product conversion using ^{19}F MRI.

The hypochlorite ion ($^{-}$OCl) is an important reactive oxygen species (ROS) in living organisms. Endogenous $^{-}$OCl is produced mainly by myeloperoxidase (MPO), a heme-containing enzyme present in neutrophils and macrophages/microglia.[1] Typically, $^{-}$OCl functions to injure pathogens oxidatively. Conversely, it is suggested that abnormal generation of $^{-}$OCl leads to tissue damage and diseases such as arthritis,[2] hepatic ischemia–reperfusion,[3] renal disease,[4] and lung injury.[5] Consequently, the demand for $^{-}$OCl-detection and -imaging probes has increased. These probes are powerful tools for understanding the biological roles of $^{-}$OCl and could also be useful for medical diagnosis.[6]

The typical $^{-}$OCl bioimaging agents are fluorescent probes that can be used in combination with fluorescence microscopy. In particular, activatable fluorescent probes,[7] which turn on fluoresce after reaction with the target species, have been developed for the direct monitoring of $^{-}$OCl in living cells.[6,7] Although fluorescent probes have advantages regarding sensitivity and spatiotemporal resolution, their use in in vivo applications is limited by the low penetration of excitation or emission light, with the exception of promising near-infrared fluorescence[8] and bioluminescence probes.[9]

Magnetic resonance (MR)-based techniques are appropriate for this purpose, because an MR probe can be detected even in deep sites of the opaque body.[10] Very recently, we have reported an $^{-}$OCl-reactive MR probe that was designed using a new concept of "atom arrangement."[10e] To the best of our knowledge, this is the first $^{-}$OCl-specific MR probe reported to date. However, the original probe has nonnegligible drawbacks that include low stability in water and low conversion yield. These were problems to be solved for future MRI studies. Under these circumstances, we were prompted to develop a superior $^{-}$OCl-specific MRI probe. Here, we report a promising candidate. The designed ^{19}F MRI probe achieved high specificity for, and reactivity with, $^{-}$OCl, and was demonstrated to have a high potentiality for the ^{19}F chemical shift-based sensing and imaging of $^{-}$OCl.

^{19}F is the most attractive of the MR-detectable nuclei because of its high sensitivity (0.83 relative to ^{1}H) and low background signal in biological samples.[11,12] We then took on the challenge of developing an $^{-}$OCl-specific ^{19}F MRI probe. Based on early reports of $^{-}$OCl-reactive chemical structures, initially we designed MRI probe **1**, which has a CF_3 group on the *p*-aminophenyl alkyl ether scaffold (Figure 1b). As demonstrated by Urano and Nagano, the *p*-aminophenyl aryl ether moiety reacts expeditiously with ROS, preferably with $^{-}$OCl, to give 1,4-benzoquinone imine by *o*-dearylation via an *ipso*-substitution mechanism (Figure 1a).[13] The utility of this moiety for designing ROS-selective probes has been well proven by its successful application to an elegant ROS-sensing fluorescent probe, i.e., aminophenyl fluorescein (APF)[13d] and sulfonaphthoaminophenyl fluorescein (SNAPF).[8a] Therefore, we assumed that the designed *p*-aminophenyl alkyl ether **1**, an analog of *p*-aminophenyl aryl ether, also reacts with ROS effectively to give 1,4-benzoquinone imine and 2-trifluoroethanol (CF_3CH_2-OH) (Figure 1b).

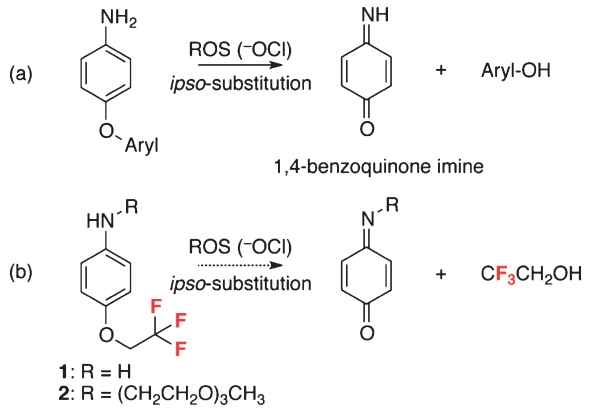

Figure 1. (a) ROS ($^{-}$OCl)-reactive *p*-aminophenyl aryl ether moiety and its proposed reaction scheme. (b) Chemical structure of the designed ^{19}F MRI probes **1** and **2**, and predicted reaction for the spontaneous production of trifluoroethanol (CF_3CH_2OH) via *ipso*-substitution. Fluorine atoms are colored in red.

First, we investigated whether probe **1** reacts with $^{-}$OCl, as proposed in Figure 1b. Reaction of **1** (100 μM) with $^{-}$OCl (200 μM) in phosphate buffer (pH 7.4, 100 mM) containing 150 mM NaCl and 0.1% DMF was evaluated using HPLC analysis (Figure S1[14]). After reaction with $^{-}$OCl, probe **1** was consumed completely to give a new product, which was converted further to *p*-aminophenol by the addition of the reducing agent $NaBH_4$. Based on the reasonable assumption that *p*-aminophenol was produced by the reduction of 1,4-benzoquinone imine, in addition to the finding that trifluoroethanol was produced as a major product (detected by ^{19}F NMR, vide infra),

 © 2011 The Chemical Society of Japan

Editor's Choice

these results support the scheme shown in Figure 1b as a major reaction mechanism. Furthermore, probe **1** reacted with $^{-}$OCl efficiently and quickly (Figure S2[14]), thus seeming suitable as an $^{-}$OCl-sensing probe. Unfortunately, however, the solubility of probe **1** in water was too low (0.73 mM at maximum in phosphate buffer pH 7.4) for its application in further biological studies.

To improve solubility, we prepared probe **2**, in which the *p*-amino group of **1** was monoalkylated by a triethylene glycol unit. During the derivatization study of **1**, we found that *N*-monoalkylation did not affect the reactivity between the *p*-aminophenyl alkyl ether and $^{-}$OCl, whereas *N*-bisalkylation suppressed the reactivity completely (data not shown). Therefore, probe **2**, which is soluble in water up to 15 mM, was $^{-}$OCl reactive. The reactivity of probe **2** with $^{-}$OCl, which was analyzed using HPLC, was very high and resulted in 80 and 100% consumption of **2** after incubation with only 1 and 2 equivalents of $^{-}$OCl, respectively. On the other hand, the probe **2** was almost intact after incubation without $^{-}$OCl, suggesting the stability of the probe under physiological conditions and good reactivity to $^{-}$OCl.

With a water-soluble and $^{-}$OCl-reactive probe in hand, we moved on to the visualization of $^{-}$OCl using ^{19}F MRI, which was the aim of the present work. ^{19}F NMR analyses of the authentic samples, probe **2** and the predicted product trifluoroethanol, gave ^{19}F signals at −75.1 and −77.7 ppm, respectively (Figure 2a). The observed ^{19}F chemical-shift difference between the probe and the product was 2.6 ppm, which was sufficient to visualize each compound separately using ^{19}F chemical-shift-selective MRI. Figure 2b depicts phantom images (11.7 T) of these compounds. ^{1}H MRI visualized both samples because of the presence of H_2O (left panel in Figure 2b). In contrast, probe **2** and the product (trifluoroethanol) were visualized separately using ^{19}F chemical-shift-selective imaging (second-right and right panels in Figure 2b, obtained based on probe **2**- and trifluoroethanol-selective ^{19}F pulse frequencies, respectively).

Then, we applied probe **2** to the detection and imaging of $^{-}$OCl in ^{19}F MR modality. After addition of $^{-}$OCl, the ^{19}F signal of probe **2** (−75.1 ppm) shifted to a new peak at −77.7 ppm, corresponding to trifluoroethanol, in a clear $^{-}$OCl-dose-dependent manner (Figure S3[14]). The comparison of ^{19}F NMR peak integrals allowed us to calculate that probe **2** (100 μM) produced trifluoroethanol with a reaction yield of 56% via a reaction with 2 equivalents of $^{-}$OCl. Because of the efficient probe-to-product conversion, this $^{-}$OCl-dose-dependent consumption of probe **2** and generation of trifluoroethanol, i.e., the presence or absence of $^{-}$OCl, was well visualized using ^{19}F chemical-shift-selective imaging (Figure S4[14]). These data indicate the utility of compound **2** as an $^{-}$OCl-imaging probe in ^{19}F MR modality.

In addition to the high reactivity and good conversion yield obtained, probe **2** also exhibited high specificity for $^{-}$OCl. HPLC analyses revealed that probe **2** remained intact after reaction with most of the biologically important ROS (H_2O_2, ROO$^{\bullet}$, $O_2^{\bullet-}$, and $^{\bullet}$OH) and reactive nitrogen species (RNS; $ONOO^{-}$), with the exception of $^{-}$OCl and NO (Figure S5[14]). However, and interestingly, the analysis of the reaction of probe **2** with ROS or RNS in ^{19}F NMR modality showed that probe **2** produced a ^{19}F NMR peak at −77.7 ppm, corresponding to trifluoroethanol, only after reaction with $^{-}$OCl (Figure 3a). Reaction with NO decreased the intensity of the ^{19}F signal at

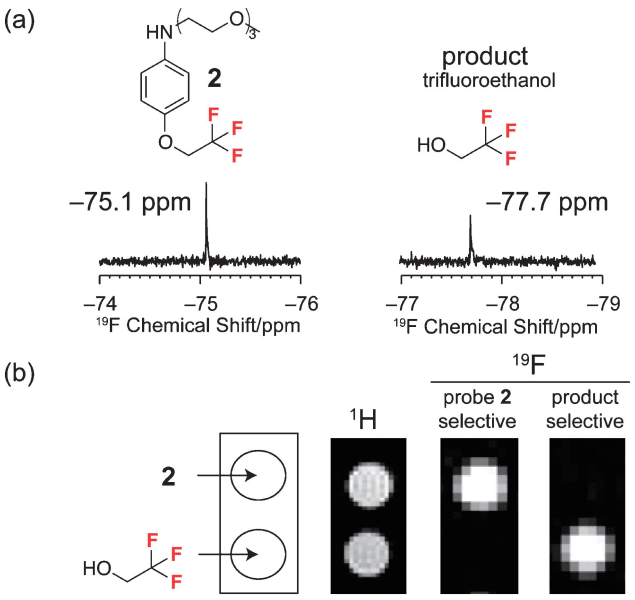

Figure 2. (a) ^{19}F NMR spectra of probe **2** and trifluoroethanol (100 μM). (b) ^{1}H and ^{19}F chemical-shift-selective imagings (11.7 T) of probe **2** and trifluoroethanol (10 mM each). Samples were dissolved in phosphate buffer (pH 7.4, 100 mM) containing 150 mM NaCl and 0.1% DMF.

−75.1 ppm (probe **2**) but produced no ^{19}F signal at −77.7 ppm (trifluoroethanol), suggesting that NO reacts with probe **2** but does *not* undergo *o*-dealkylation via an *ipso*-substitution pathway.

Because of the $^{-}$OCl-specific production of trifluoroethanol, as described above, probe **2** yielded targeted imaging of $^{-}$OCl (Figure 3b). ^{19}F chemical-shift-selective imaging (trifluoroethanol ^{19}F selective) gave a clear signal for probe **2** only in the presence of $^{-}$OCl (bottom panel in Figure 3b). The specificity of the reaction was high; the presence of other ROS or RNS produced no such signals. These results show clearly that the designed compound **2** functions as a ^{19}F MRI probe for the highly specific detection and imaging of $^{-}$OCl.

In conclusion, we designed an $^{-}$OCl-sensing ^{19}F MRI probe. The advantages of this probe were at least threefold. The first advantage was reactivity. The probe, which contained a *p*-aminophenyl alkyl ether scaffold, reacted expeditiously with $^{-}$OCl to produce trifluoroethanol with a high conversion yield. The second advantage was specificity. The probe produced trifluoroethanol only after reaction with $^{-}$OCl. The third advantage was its applicability to ^{19}F MRI. Because of the sufficient ^{19}F chemical-shift change concomitant with probe-to-product conversion, $^{-}$OCl was detected and visualized using ^{19}F chemical-shift-selective imaging. To the best of our knowledge, this is the first MRI probe that yields $^{-}$OCl imaging with a high specificity among a variety of ROS and RNS. Our next challenge is to adapt the probe to in vivo applications, e.g., evaluation, optimization, and improvement of the biodistribution or biokinetics of the probe. Along these lines, and in addition to the ^{19}F MRI application described here, ^{19}F MR spectroscopy using a much larger voxel, which could provide the possibility for probe/product ratiometric analysis, may also be a promising target of this probe. Further work is now underway in our laboratory.

 © 2011 The Chemical Society of Japan

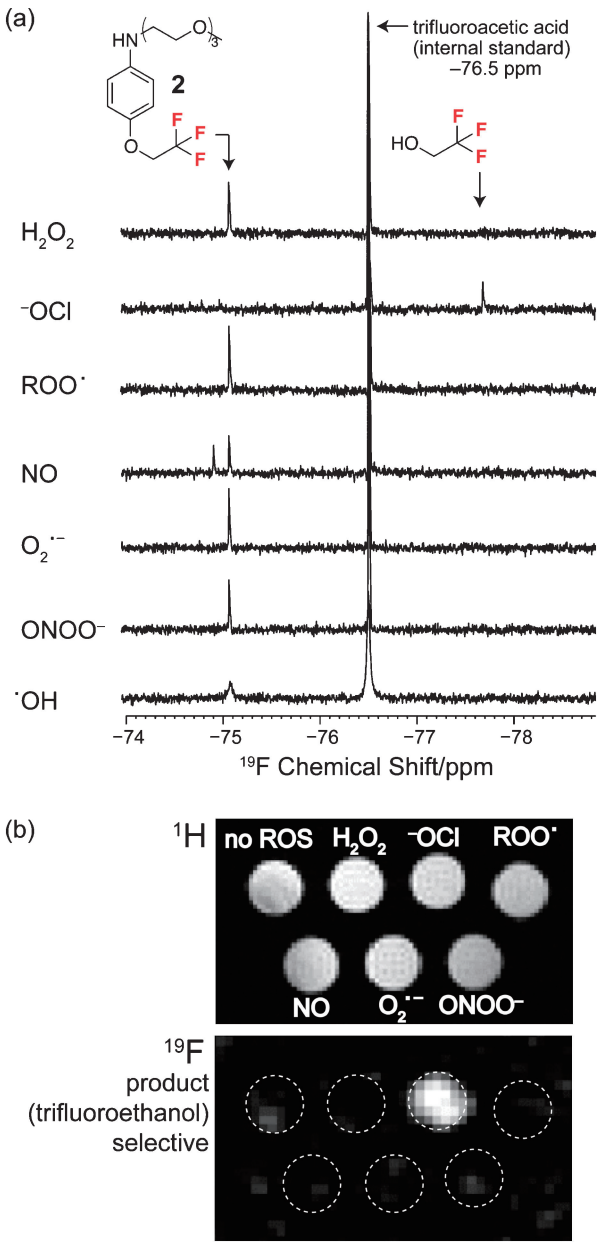

Figure 3. (a) ^{19}F NMR spectra of probe **2** (100 μM) after reaction with the various ROS and RNS indicated on the left side of spectra. Each ROS or RNS was generated according to the typical procedure described in ESI. H_2O_2: H_2O_2 solution (final 200 μM), $^-$OCl: NaOCl solution (final 200 μM), ROO$^\bullet$: 2,2′-azobis(2-amidinopropane) dihydrochloride solution (final 200 μM; one reagent produces two ROO$^\bullet$, so that final concentration of ROO$^\bullet$: 400 μM), NO: NOC7 solution (final 100 μM; one NOC7 produces two NO, so that the final concentration of NO: 200 μM)), $O_2^{\bullet-}$: solid KO_2 (final 200 μM), $ONOO^-$: $ONOO^-$ solution (final 200 μM), and $^\bullet$OH: $Fe(ClO_4)_2$ (final 1 mM) + H_2O_2 (final 9.7 mM). ^{19}F peak of the probe after reaction of $^\bullet$OH was broadened (bottom spectrum). This is highly likely because Fe^{3+} ion, produced during the generation of $^\bullet$OH, induces a paramagnetic relaxation effect. (b) (top) ^{1}H and (bottom) ^{19}F chemical-shift-selective imagings (11.7 T, ^{19}F of trifluoroethanol selective) of ROS and RNS using probe **2**. Samples were prepared according to the procedure described in (a), but using 100 times higher concentrations of probe and ROS or RNS. Because the Fe^{3+} ion, which is produced by the Fenton reaction used for generation of $^\bullet$OH, perturbs MRI, $^\bullet$OH was omitted from the ROS and RNS tested.

We thank Prof. Masahiro Shirakawa of Kyoto University for his help on ^{19}F MRI measurements. This work was supported by the NEXT Program, a Grant-in-Aid (No. 22685018) from JSPS, Japan and partly by the Innovative Techno-Hub for Integrated Medical Bio-Imaging Project from MEXT, Japan and the Global COE Program "Science for Future Molecular Systems".

References and Notes

1 J. E. Harrison, J. Schultz, *J. Biol. Chem.* **1976**, *251*, 1371.
2 a) H. E. Jasin, *Inflammation* **1993**, *17*, 167. b) S. M. Wu, S. V. Pizzo, *Arch. Biochem. Biophys.* **2001**, *391*, 119.
3 T. Hasegawa, E. Malle, A. Farhood, H. Jaeschke, *Am. J. Physiol.: Gastrointest. Liver Physiol.* **2005**, *289*, G760.
4 E. Malle, T. Buch, H.-J. Grone, *Kidney Int.* **2003**, *64*, 1956.
5 S. Hammerschmidt, N. Büchler, H. Wahn, *Chest* **2002**, *121*, 573.
6 For a recent review on ROS or RNS imaging fluorescent probes, see: T. Nagano, *J. Clin. Biochem. Nutr.* **2009**, *45*, 111, and references therein.
7 For a recent review on activatable probes, see: H. Kobayashi, M. Ogawa, R. Alford, P. L. Choyke, Y. Urano, *Chem. Rev.* **2010**, *110*, 2620, and references therein.
8 a) J. Shepherd, S. A. Hilderbrand, P. Waterman, J. W. Heinecke, R. Weissleder, P. Libby, *Chem. Biol.* **2007**, *14*, 1221. b) P. Panizzi, M. Nahrendorf, M. Wildgruber, P. Waterman, J.-L. Figueiredo, E. Aikawa, J. McCarthy, R. Weissleder, S. A. Hilderbrand, *J. Am. Chem. Soc.* **2009**, *131*, 15739. c) Y. Koide, Y. Urano, K. Hanaoka, T. Terai, T. Nagano, *J. Am. Chem. Soc.* **2011**, *133*, 5680.
9 S. Gross, S. T. Gammon, B. L. Moss, D. Rauch, J. Harding, J. W. Heinecke, L. Ratner, D. Piwnica-Worms, *Nat. Med.* **2009**, *15*, 455.
10 For ROS-sensitive MR probes, see: a) J. W. Chen, W. Pham, R. Weissleder, A. Bogdanov, Jr., *Magn. Reson. Med.* **2004**, *52*, 1021. b) H. Utsumi, K.-i. Yamada, K. Ichikawa, K. Sakai, Y. Kinoshita, S. Matsumoto, M. Nagai, *Proc. Natl. Acad. Sci. U.S.A.* **2006**, *103*, 1463. c) E. Rodríguez, M. Nilges, R. Weissleder, J. W. Chen, *J. Am. Chem. Soc.* **2010**, *132*, 168. d) A. R. Lippert, K. R. Keshari, J. Kurhanewicz, C. J. Chang, *J. Am. Chem. Soc.* **2011**, *133*, 3776. e) T. Doura, H. Nonaka, S. Sando, *Chem. Commun.* **2012**, in press. doi:10.1039/C1CC12044A.
11 a) J.-x. Yu, V. D. Kodibagkar, W. Cui, R. P. Mason, *Curr. Med. Chem.* **2005**, *12*, 819. b) S. L. Cobb, C. D. Murphy, *J. Fluorine Chem.* **2009**, *130*, 132.
12 For recent examples of ^{19}F NMR probes, see: a) S. Mizukami, R. Takikawa, F. Sugihara, Y. Hori, H. Tochio, M. Wälchli, M. Shirakawa, K. Kikuchi, *J. Am. Chem. Soc.* **2008**, *130*, 794. b) B. J. Stockman, *J. Am. Chem. Soc.* **2008**, *130*, 5870. c) J.-X. Yu, V. D. Kodibagkar, L. Liu, R. P. Mason, *NMR Biomed.* **2008**, *21*, 704. d) K. Tanabe, H. Harada, M. Narazaki, K. Tanaka, K. Inafuku, H. Komatsu, T. Ito, H. Yamada, Y. Chujo, T. Matsuda, M. Hiraoka, S.-i. Nishimoto, *J. Am. Chem. Soc.* **2009**, *131*, 15982. e) Y. Takaoka, T. Sakamoto, S. Tsukiji, M. Narazaki, T. Matsuda, H. Tochio, M. Shirakawa, I. Hamachi, *Nat. Chem.* **2009**, *1*, 557. f) K. Yamaguchi, R. Ueki, H. Nonaka, F. Sugihara, T. Matsuda, S. Sando, *J. Am. Chem. Soc.* **2011**, *133*, 14208.
13 a) Y. Urano, T. Higuchi, M. Hirobe, *J. Chem. Soc., Perkin Trans. 2* **1996**, 1169. b) Y. Urano, T. Higuchi, M. Hirobe, T. Nagano, *J. Am. Chem. Soc.* **1997**, *119*, 12008. c) K.-i. Setsukinai, Y. Urano, K. Kikuchi, T. Higuchi, T. Nagano, *J. Chem. Soc., Perkin Trans. 2* **2000**, 2453. d) K.-i. Setsukinai, Y. Urano, K. Kakinuma, H. J. Majima, T. Nagano, *J. Biol. Chem.* **2003**, *278*, 3170.
14 Supporting Information is available electronically on the CSJ-Journal Web site, http://www.csj.jp/journals/chem-lett/index.html.

 © 2011 The Chemical Society of Japan